DYNAMIC ANALYSIS OF SHELLS USING DOUBLY-CURVED FINITE ELEMENTS

B. E. Greene, R. E. Jones, R. W. McLay*,
and D. R. Strome

The Boeing Company
Aerospace Systems Division
Seattle, Washington

This paper discusses the theoretical development of a computer program for the static and dynamic analysis of general shell structures. The theory is based on the finite element concept and uses both the generalized finite element method and the direct stiffness approach for the forming of the pertinent equations. The treatment of shell surface geometry, the displacement functions and elemental degrees of freedom, and the modification of the generalized stiffness method required for the implementation of the triangular element are described. The correlation of both theoretical and experimental results with those obtained by the present method are shown along with idealizations required for accurate results. Static and dynamic solution results are compared.

Research supported by the Air Force Flight Dynamics Laboratory, AFSC under Contract F33615-67-C-1661.

*Associate Professor of Mechanical Engineering, University of Vermont, Burlington, Vermont (formerly Research Specialist, The Boeing Company, Seattle, Washington)

Report Documentation Page

Form Approved
OMB No. 0704-0188

1. REPORT DATE	2. REPORT TYPE	3. DATES COVERED
OCT 1968		**00-00-1968 to 00-00-1968**

4. TITLE AND SUBTITLE	5a. CONTRACT NUMBER
Dynamic Analysis of Shells Using Doubly-Curved Finite Elements	5b. GRANT NUMBER
	5c. PROGRAM ELEMENT NUMBER
6. AUTHOR(S)	5d. PROJECT NUMBER
	5e. TASK NUMBER
	5f. WORK UNIT NUMBER
7. PERFORMING ORGANIZATION NAME(S) AND ADDRESS(ES) **Air Force Flight Dynamics Laboratory,Wright Patterson AFB,OH,45433**	8. PERFORMING ORGANIZATION REPORT NUMBER
9. SPONSORING/MONITORING AGENCY NAME(S) AND ADDRESS(ES)	10. SPONSOR/MONITOR'S ACRONYM(S)
	11. SPONSOR/MONITOR'S REPORT NUMBER(S)

12. DISTRIBUTION/AVAILABILITY STATEMENT
Approved for public release; distribution unlimited

13. SUPPLEMENTARY NOTES
See also AD0703685, Proceedings of the Conference on Matrix Methods in Structural Mechanics (2nd) Held at Wright-Patterson Air Force Base, Ohio, on 15-17 October 1968.

14. ABSTRACT

15. SUBJECT TERMS

16. SECURITY CLASSIFICATION OF:			17. LIMITATION OF ABSTRACT	18. NUMBER OF PAGES	19a. NAME OF RESPONSIBLE PERSON
a. REPORT	b. ABSTRACT	c. THIS PAGE			
unclassified	**unclassified**	**unclassified**		**28**	

SECTION I

INTRODUCTION

The research reported in this paper represents a portion of the work accomplished under Contract No. F33615-67-C-1661, sponsored by the Flight Dynamics Laboratory, Wright-Patterson Air Force Base. The contract work has as its goal the development, application, and evaluation of doubly-curved finite elements in the dynamic analysis of shells. It has encompassed the development of stiffness and mass matrices for shell elements on a doubly curved surface. The shell geometry is limited only by the condition that the surface equations be given in the parametric form

$$x = f_1(\alpha_1, \alpha_2)$$

$$y = f_2(\alpha_1, \alpha_2)$$

$$z = f_3(\alpha_1, \alpha_2)$$

in which f_1, f_2, f_3 are known functions of the parameters α_1 and α_2, and the latter constitute an orthogonal, principal curvilinear coordinate system on the surface of the shell.

Derivation of the shell element stiffness matrices is based on the strain displacement equations of Novozhilov, Reference 1, while the elemental mass matrices are derived by classical means from the kinetic energy associated with the admissible displacement states as described by Archer, Reference 2.

Two basic element planforms are considered; one is a quadrilateral bounded by principal coordinate lines (hence, a "rectangle" in the orthogonal, curvilinear coordinate system), and the other is a triangle with arbitrarily oriented sides. Supplementary to these two basic shell elements there has also been developed an apex element, which is a degenerate case of the quadrilateral. It is obtained by modifying the quadrilateral element to make it suitable for use at the apex of a shell of revolution, where there is a pole in the surface coordinate system. A stiffener element lying on a meridonal or circumferential coordinate line of a surface of revolution has also been developed. This element has stretching, bending, and torsional properties, and its elastic axis may be offset from the middle surface of the shell.

To apply the finite elements just described to the analysis of actual shell problems, a computer code has been developed. The code generates, from basic input data describing the geometry, material, and loading of the shell, the elemental stiffness, mass, and loads matrices for the above elements, and assembles them into gross matrices representing the linear, undamped equations of motion of the complete shell. These equations are solved for static deflections of the shell and for natural vibration modes and frequencies.

Evaluation of the shell finite element analysis is being accomplished by correlating the results obtained from the computer code described above for several specific shell response problems, both static and dynamic, with exact theoretical solutions, experimental data, or other numerical solutions.

The purpose of this paper is to describe briefly the methods developed and to demonstrate their validity by presenting the correlation studies which have been completed at this time. The description of the methods is limited to what are considered the most important concepts, which include the treatment of the shell surface geometry, the displacement functions and elemental degrees of freedom, and the modifications to the existing finite element technology which are required for the implementation of the triangular element. Numerical results for shells analyzed using stiffener elements and triangular shell elements are not available at the time of writing this paper; therefore, the examples presented are limited to unstiffened shells and to the use of quadrilateral elements.

More detailed descriptions of the methods developed, including detailed element derivations, will appear in the contract final report, which will be completed later this year.

SECTION II

SHELL ELEMENT GEOMETRY

The computer code must be applicable to a very wide range of doubly or singly curved shells. In the computation process, an approximate shell geometry must be defined from given input data. Because of the great variety of shell shapes and the rather complex forms of their geometrical descriptions, in terms of a set of interrelated mathematical functions, this geometrical definition is a difficult task. There are two alternative procedures which could be used. The first is the construction of an assemblage of shell elements which fits together in a continuous fashion and is a close approximation to the shape of the actual shell. This almost certainly would require a matching of nodal locations between the element assemblage and the actual shell. It should also include a matching of the two slope components at each node. Hopefully, each element of the assemblage could have a relatively simple doubly curved shape. This approach is extremely difficult, in general, for the reason that simple element shapes do not permit sufficiently continuous assemblages for actual shells of a wide range of shapes. The second procedure is to approximate, in a physical way, the shell itself. The geometrical functions which are approximated are the Lamé parameters, A_1, A_2, and A_{12}, which determine length and angle relationships in the shell middle surface, and the radii of curvature, R_1, R_2, and the twist, R_{12}, which determine the local departure of the shell from planeness. By representing these functions by approximate forms, such as polynomials, in the shell middle surface coordinate system, a close approximation to the actual shell is obtained in a numerical sense. However, the approximate functions do not represent any actual shell at all; that is, they do not necessarily satisfy the surface compatibility equations of Gauss and Codazzi.

In addition to the six quantities listed above, their derivatives with respect to the surface coordinates, as well as the shell thickness, t, appear as products in various combinations within the terms of the strain energy integral. To evaluate the energy accurately, each such term should be approximated individually, starting with the true shell functions, rather than by taking derivatives and forming products of approximate functions already defined.

The purpose of the geometrical representation is to make possible the evaluation of the strain energy integral for the shell elements. It is believed that an accurate evaluation of the strain energy function is more important than adherence to a true shell surface, composed of elements each of which may depart significantly in local geometry from the actual shell. For this reason, the second approach has been used.

All derivations and calculations have been based on the use of a principal coordinate system in the shell middle surface, defined by the variables α_1 and α_2. In this case A_{12} and R_{12} vanish, and R_1, R_2 are the principal radii of curvature of the mid-surface. The necessary actual shell description for problem solutions consists of the functions (either in mathematical or dense tabular form) A_1, A_2, R_1, R_2, and t in terms of the principal coordinates of the surface. In addition, it is necessary to have a description of the principal coordinate system in terms of a base rectangular cartesian reference frame, in order to determine the locations of loadings, nodes, etc., in terms of α_1 and α_2. The approximations to the terms of the strain energy integral, in terms of α_1 and α_2, are second degree polynomials determined by matching the individual function values at points on the boundaries and in the interior of the elements.

SECTION III

SHELL ELEMENT DISPLACEMENT FUNCTIONS

The element displacement functions were chosen on the basis of an accumulation of requirements which has gradually taken shape as a result of the work of a number of researchers. It appears worthwhile to discuss this accumulation of knowledge here, since such a summary has not been given previously.

1. The rigid body motion of an element must be represented, at least approximately, in the displacement functions. This item has been the subject of some controversy. Jones and Strome, (Reference 3), included rigid motions explicitly in their doubly curved shell element and found a gain in accuracy to occur. Cantin and Clough, (Reference 4) found similar results in their cylindrical shell element. On the other hand, Bogner, Fox, and Schmidt, (Reference 5) obtained excellent results with a cylindrical shell element without explicit inclusion of rigid motions. Haisler and Stricklin, (Reference 6) also presented data supporting the omission of rigid modes. The conclusion which appears to derive from all work to date is that rigid motions must be represented, but that this can be done adequately by means of polynomial displacement functions of sufficiently high degree.

2. The functions u, v, and w should all be represented with equal accuracy, i.e., by polynomials of equal degree. The basis of this is also contained in the work of a number of authors. Jones and Strome found that the explicit inclusion of the rigid body displacements was insufficient to provide either a high level of accuracy for large element sizes or a rapid convergence with decreasing element sizes. In order to obtain such results, they found it necessary to add two other displacement forms. These amounted to explicit inclusion of uniform hoop expansion and rotation of an axisymmetric element about its own circumferential central circle, similar in nature to torsion of a ring. These functions had the effect of increasing the degree of the displacement polynomials, primarily the tangential displacement function, which initially had been of the first degree in the arc length variable. With these functions, good accuracy has been obtained for elements of very large size. The Haisler and Stricklin element has the same polynomial functions as the initial polynomial of Jones and Strome. It has shown relatively slow convergence and the need for small elements to obtain good accuracy. The Cantin and Clough displacements and those of Bogner, Fox, and Schmidt differ only in the use, in the former, of a bilinear polynomial for u and v, compared to a bicubic polynomial in the latter. The Bogner, et. al., element shows much faster convergence and better accuracy for large elements than that of Cantin and Clough. Similar conclusions arise from the results of Greene, et. al., (Reference 7). Based on these results, the need for equally competent forms for all of u, v, and w appears to be justified.

3. The displacement functions for u, v, and w should be at least of the competence of the bicubic form

$$\sum_{m=1}^{4} \sum_{n=1}^{4} A_{mn} f_m(\alpha_1) g_n(\alpha_2)$$

where f_m and g_n are descriptively called beam functions. That is, each is a cubic polynomial and defines the displacement within a line element in terms of the displacement and slope at its ends. They provide the ability of each function of α_1, i.e., $f_m(\alpha_1)$, to build up and die out in the α_2 direction in one element span, and vice versa.

Several investigators have independently discovered the bicubic functions, but most have applied it incorrectly or in an incomplete form. The correct form and usage is given for plate elements in Reference 8 and for cylindrical shell elements in Reference 5. Results of good accuracy were obtained in this work. Based on this and on similar results obtained by Greene, et. al., the bicubic functions have been adopted for the present work on doubly curved shells.

4. The continuity of displacement and slope must be enforced, at least approximately, at the interelement boundaries. This requirement has been discussed by a number of investigators. It was covered most completely in the work of Greene, et. al., where it was found that exact continuity need not be enforced to obtain good accuracy. Instead, with competent (reasonably high degree) displacement functions, good accuracy can be obtained with continuity enforced only on the lower degree polynomial components of the displacements and slopes at the interelement boundaries. The bicubic forms provide the ability to obtain exact continuity for shell elements whose corners are right angles, provided that the radius of curvature is continuous across interelement boundaries. An ingenious set of functions which satisfies explicitly all continuity requirements for a flat triangular plate element is given in References 9 and 10. Its extension to a doubly curved shell element appears at the present to be quite complicated, and therefore, for triangular elements it was decided to apply the generalized finite element approach, using Lagrange multiplier functions to enforce approximate continuity. This was described by Jones, (Reference 11) and applied by Greene, et. al., (Reference 7). An extension of this approach was given by McLay, (Reference 12) which greatly increases its applicability to the practical solution of problems.

The displacement functions used for each of u, v, and w, are cubic polynomials in two variables,

$$\sum_{m=0}^{3} \sum_{n=0}^{3} B_{mn} \xi^m \zeta^n$$

where ξ and ζ are, respectively, dimensionless variables representing α_1 and α_2 and having unit change over the total dimensions of the element. The element matrix derivations are carried out in the terms of the coefficients B_{mn}, and are then transformed by invariance to the more physically convenient coefficients, A_{mn}, of the previously given displacement form. This procedure makes it convenient to carry out the derivation of the stiffness matrix in closed form, a single algebraic expression being obtained for each of the six distinct partitions of the matrix when it is partitioned according to u, v, and w displacement fields. The transformed degrees of freedom, A_{mn}, include at each node of a quadrilateral element for each of u, v, and w, its value, its derivative with respect to each of ξ and ζ, and its second cross derivative with respect to ξ and ζ. These total 48 degrees of freedom per element. By matching between elements common to a node all of the 12 degrees of freedom per node, complete continuity of displacements and their first derivatives is obtained at all interelement boundaries. The continuity of the derivatives of u and v is not required, however, for potential energy formulations such as the finite element method. For this reason, and because the present work is aimed at stiffened shells, in which the derivatives of u and v should actually experience jumps at element boundaries where stiffeners are attached,

these derivatives are not made continuous. Omitting this requirement is accomplished by omitting the nodal matching of $\frac{\partial^2 u}{\partial \xi \partial \zeta}$ and $\frac{\partial^2 v}{\partial \xi \partial \zeta}$ between neighboring elements. These degrees of freedom are handled by eliminating them at the elemental level. They become dependent freedoms, determined by the values of the remaining 40 freedoms of the element. All of the latter freedoms are merged, that is, matched between elements, at the nodes. The method of Guyan, (Reference 13) is used for the corresponding reduction of the mass matrix.

The difference between the displacement functions used here and those of Reference 5 lies in the omission here of the requirement of continuity of the u and v derivatives and in the transformation to the more physically appropriate freedoms of rotations and twist of the shell at the nodes rather than simply the derivatives of u, v, and w. The latter step is necessary to preserve the continuity of slope when the curvatures of the shell may be discontinuous across interelement boundaries. It is also helpful in merging stiffener element freedoms with those of the shell.

The above discussion applies primarily to rectangular shell elements, which are expected to form the bulk of the elements in problems. Triangular elements will be used where needed, such as around cutouts or at boundaries inclined to the coordinate lines. They will be used only in conjunction with a primary system of rectangular elements and, consequently, it is most convenient to use the same displacement functions for the triangles as for the rectangles. This permits exact enforcement of continuity requirements where a triangle joins a rectangle and approximate enforcement of continuity, through the generalized method, where two triangles join.

Though numerical results for the triangular elements are not included in this paper, a brief discussion of the approximate continuity enforcement appears to be pertinent. It is given in the next section.

SECTION IV

GENERALIZED FINITE ELEMENT TECHNIQUE

The triangular elements necessarily have two corners where the sides do not meet at right angles. Because of this, it is very difficult, perhaps impossible, for doubly curved elements to maintain the required continuities of both displacement and slope across inter-element boundaries. In addition, the triangular elements, having one less node than the quadrilaterals, do not provide through nodal quantities a complete definition of the bicubic displacement forms. The generalized finite element technique provides a means for enforcing approximate continuity along the sides of adjacent elements, where exact continuity is impossible or cannot be enforced through the matching of nodal quantities. The method involves formulating the finite element equations without including explicit continuity enforcement, and subsequently imposing continuity through the use of Lagrange multiplier functions and integral constraint equations. The constraint equations are solved along with the usual finite element equations. The integral constraints can provide exact continuity if this is possible; otherwise approximate continuity is obtained.

The generalized technique has the disadvantage that it populates almost completely the mass and stiffness matrices. Since the sparseness of these matrices in usual finite element formulations is a great advantage in computing ease and economy, the generalized technique is not readily applicable in its originally given form, Reference 11. A modification of the method has been developed by McLay, (Reference 12) which eliminates this difficulty. It creates a set of imaginary lines which lie between the sides of adjacent elements where Lagrange multipliers are to be used to enforce continuity. These lines, called buffer lines, are given degrees of freedom which are defined by rotations and displacements of their end points. The deformations and displacements of the buffer lines are defined by these end points, or nodal, degrees of freedom. These nodal values become the actual freedoms of the finite element formulation. The element displacement coefficients are matched to the buffer line nodal freedoms through the use of Lagrange multipliers and thereby eliminated from the calculations. The resulting formulation has loosely coupled mass and stiffness matrices as in the usual finite element formulation. It provides, approximately or exactly, depending on the item in question, the required continuities of the finite element method.

SECTION V

DISCUSSION OF NUMERICAL RESULTS

In order to demonstrate the capability of the shell elements to model accurately shell-like structures, correlations with analytical and experimental data are given for several static and dynamic problems.

HEMISPHERICAL SHELL

The first problem considered involves edge bending behavior of a shell of revolution. A hemispherical shell was subjected to an edge radial shear load as shown in Figure 1. For the particular geometry chosen, the region of stress and deformation is confined to a 15-degree segment near the boundary. To cover adequately this region, a 30-degree segment was used in the analysis. Figure 1 shows the normal displacement and rotation respectively for three different finite element idealizations. The idealizations are: three elements at 10 degrees each, six elements at five degrees each, and 12 elements at two and one half degrees each. The figure shows that all three idealizations yield results of essentially equivalent accuracy. The results at the base of the shell are compared with the theoretical solutions given in References 1 and 14. Excellent accuracy is obtained, as seen in Table 1.

TABLE 1

PERCENT ERRORS AT BASE OF SHELL - SHELL COMPUTER PROGRAM RESULTS COMPARED TO THEORETICAL SOLUTION

IDEALIZATIONS	NORMAL DISPLACEMENT	SLOPE CHANGE
3 Elements at 10^{o}	-4.95 %	-0.16 %
6 Elements at 5^{o}	-1.98 %	-0.30 %
12 Elements at $2\text{-}1/2^{o}$	-0.22 %	-0.12 %

ELLIPSOIDAL SHELL

Previous results with curved finite element shell solutions, Jones and Strome, (Reference 3) have shown that accuracy may deteriorate seriously for shell shapes other than spherical, particularly for large elements or inadequate displacement functions. In order to demonstrate the applicability of the curved shell elements for such shells, a 2:1 ellipsoid is considered. Figure 2 shows comparative results for normal displacement and rotation from membrane theory, from the curved shell of revolution element of Reference 3, and from two

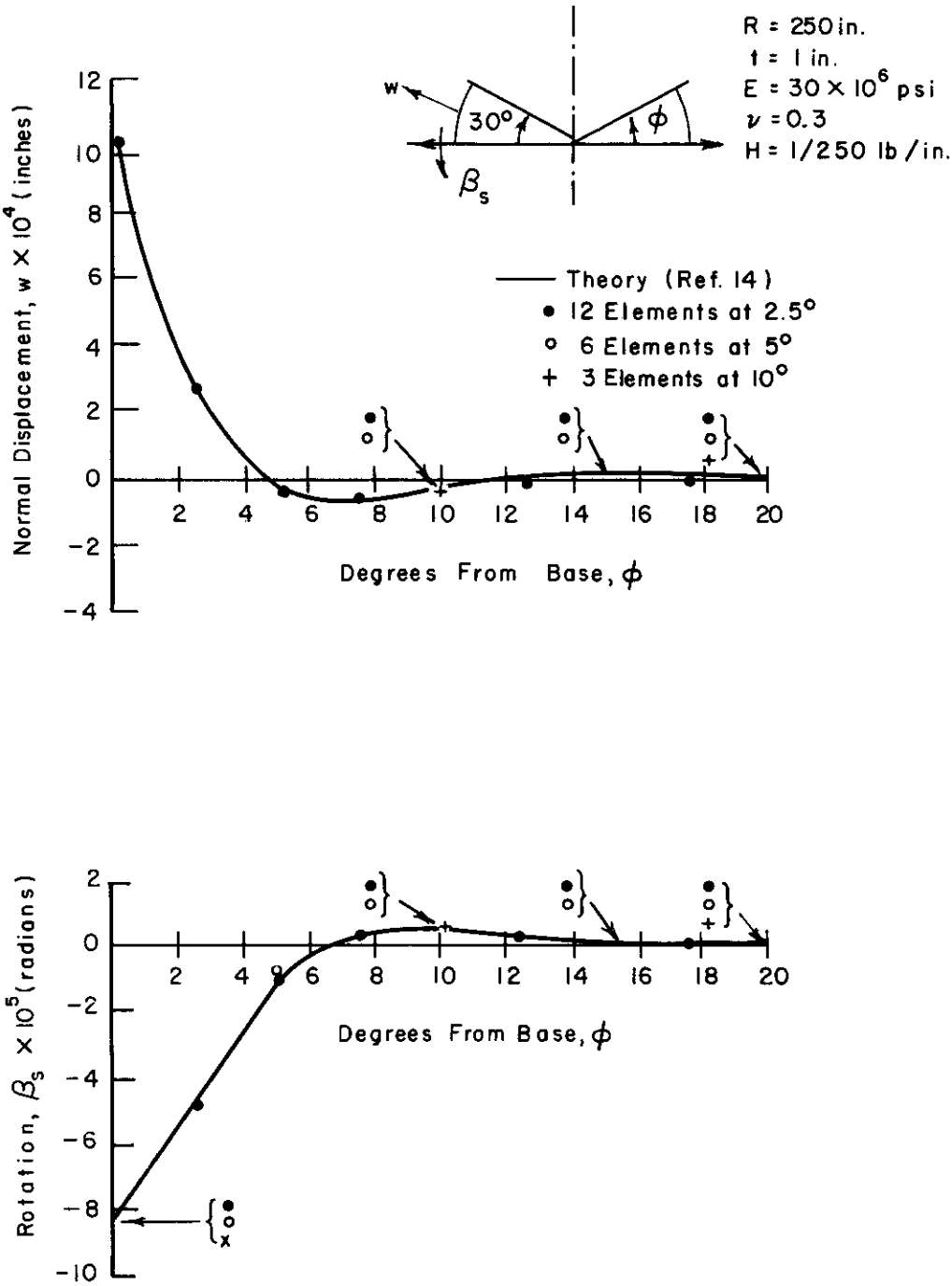

Figure 1. Normal Displacement and Rotation of a Hemispherical Shell Due to Edge Shear Load

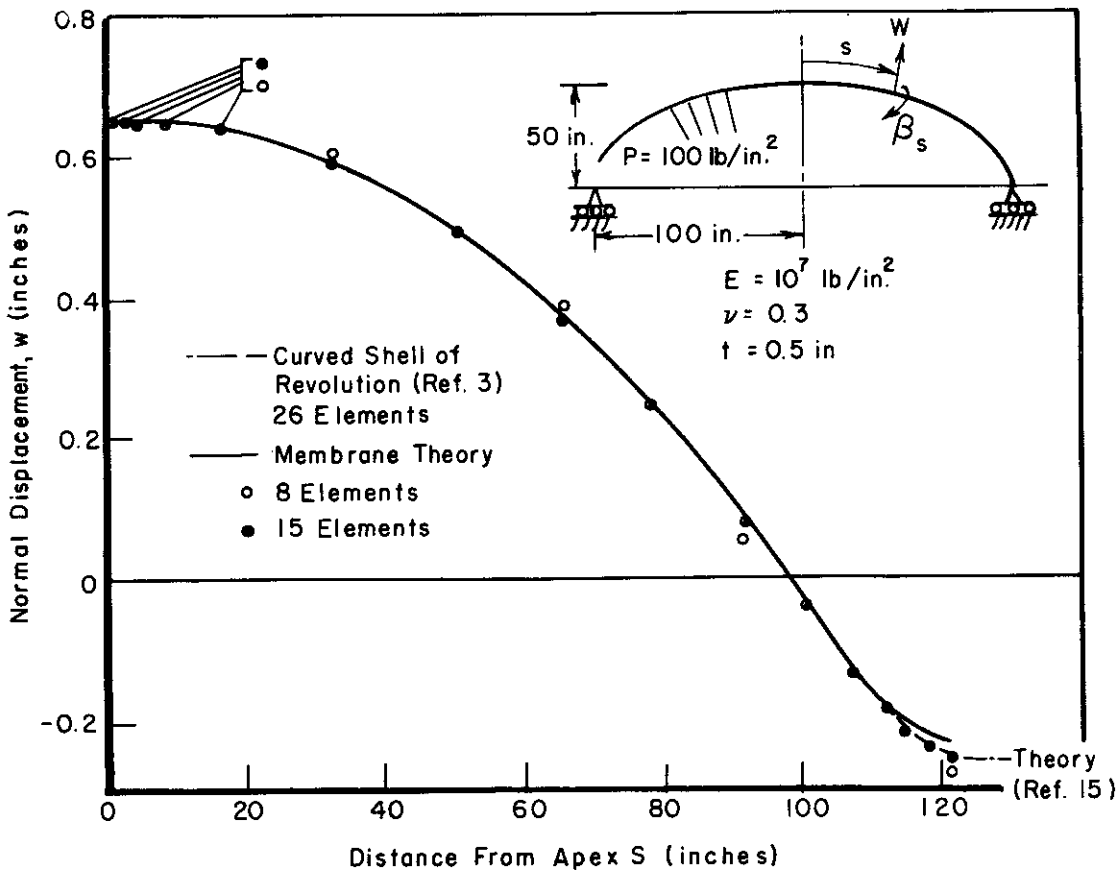

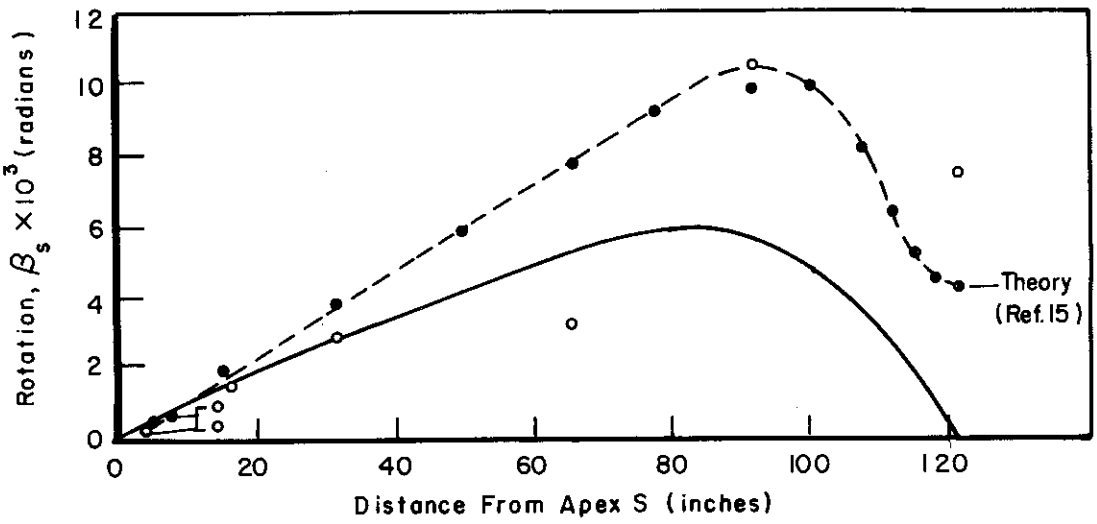

Figure 2. Normal Displacements and Rotations of an Internally Pressurized Ellipsoidal Shell

idealizations of the quadrilateral shell elements discussed in this paper. The ellipsoidal shell is loaded by internal pressure and allowed to rotate at the supports. The shell exhibits predominantly membrane behavior. However, the bending theory is required to compute the rotation of the meridional tangent. Figure 2 shows the excellent agreement of all solutions for normal displacement, and the inadequacy of the membrane theory and the eight-element quadrilateral shell idealization for predicting the rotations. The shell of revolution element of Reference 3 and the 15-element quadrilateral element solutions are essentially identical and yield excellent correlation at the boundary with the available analytical data. The latter are given in Reference 15. Comparison of finite element and exact data is given in Table 2.

TABLE 2

NORMAL DISPLACEMENT AND ROTATION AT BASE OF INTERNALLY PRESSURIZED ELLIPSOIDAL SHELL

	Theory Ref. 15	Membrane Theory	Shell of Revolution Ref. 3	Finite Element Solution	
				8 Elements	15 Elements
$w \sim$ inches	-.24048	-.230	-.24048	-.24675	-.24088
$\beta_s \sim$ radians	4.4024×10^{-4}	0	4.4341×10^{-4}	7.4940×10^{-4}	4.4217×10^{-4}

VIBRATION OF A CYLINDER

The natural frequencies and modes of a simply supported circular cylinder without axial restraint have been studied using the quadrilateral curved shell element. The configuration of the cylinder analyzed is given in Figure 3. Theoretical solutions for the natural frequencies of this cylinder presented by Voss in Reference 16 are compared with the results from the finite element analysis.

In the first study a single mode was examined. This was done by representing only one quarter-wave segment of the shell in the finite element analysis and imposing kinematic boundary conditions at the edges of this segment which are compatible with the symmetry or antisymmetry of the structural response as indicated in Figure 3.

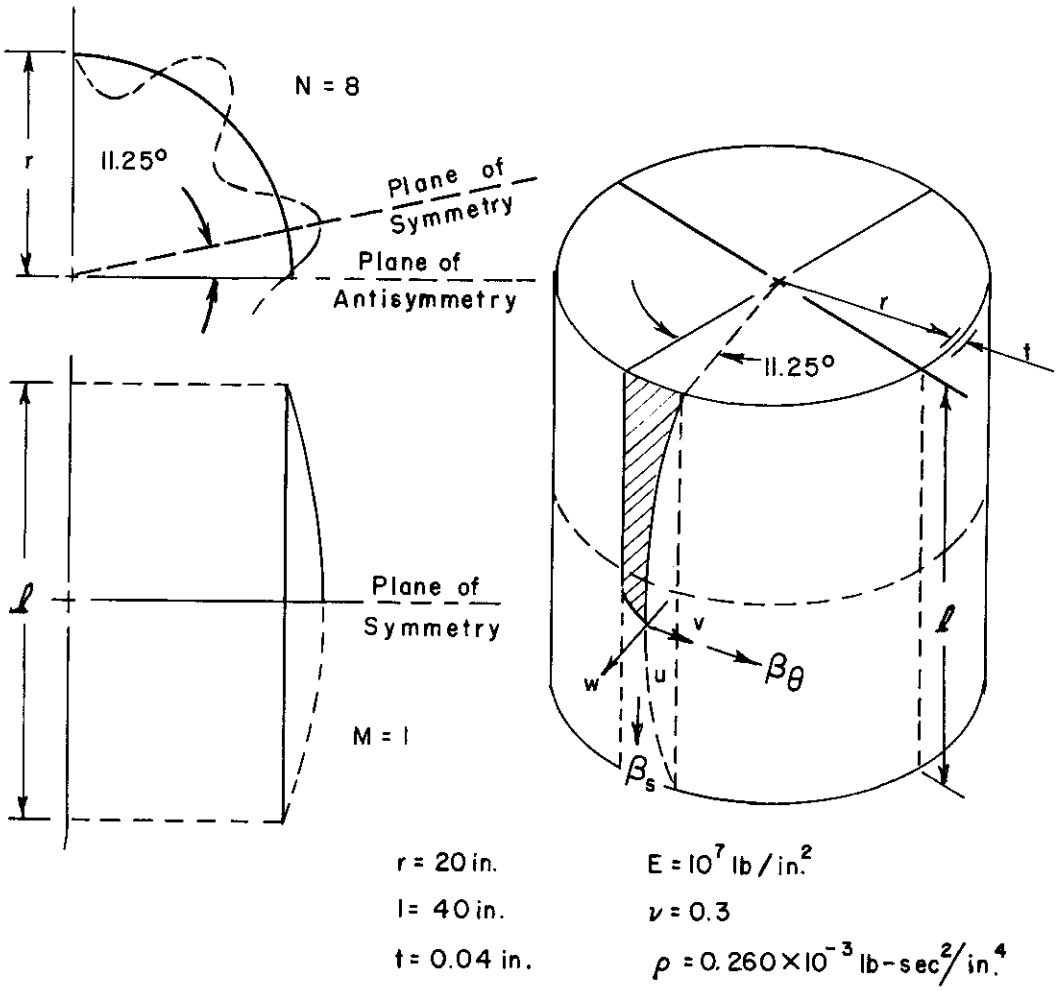

Figure 3. Analyzing a Specific Vibration Mode by Using One Quarter-Wave Segment of Shell

The purpose of this study is to examine the effects of different element size-to-wavelength ratios and different ways of distributing the mass upon the accuracy of the analysis. The mode examined is the N = 8, M = 1 mode which has eight full waves around the circumference of the cylinder and one-half wave down the length as indicated in Figure 3. This mode was selected because it is the fundamental (i.e., lowest frequency) mode for this cylinder thus assuring that it would be obtained first in the eigenvalue - eigenvector solution of the equations of motion rather than some higher order mode having the same boundary conditions. The three different idealizations of the quarter-wave segment of the shell which were analyzed consisted of one, four, and nine elements as shown in Figure 4, which also shows the boundary conditions imposed at the edges of the segment.

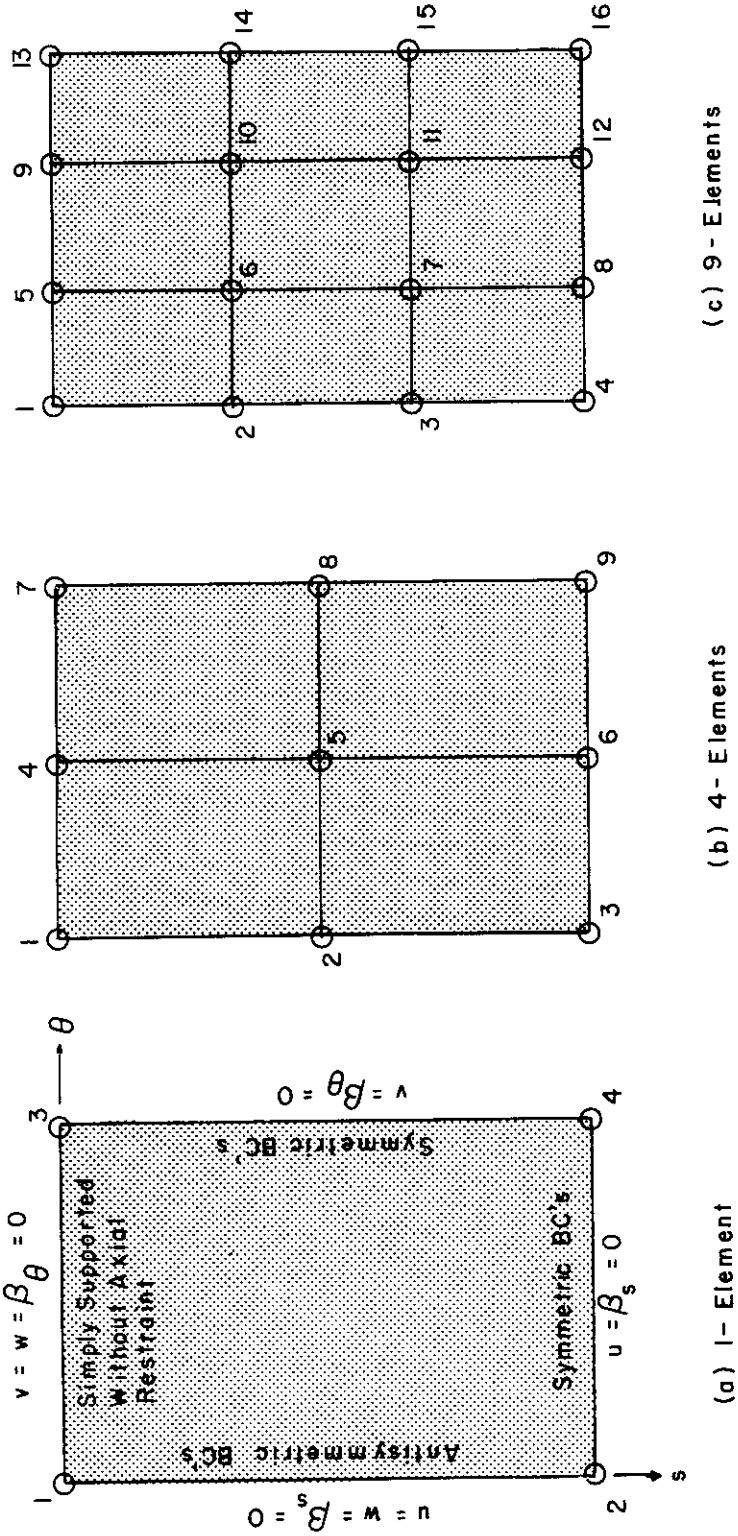

Figure 4. Idealization of Quarter-Wave Segment of Shell Showing Boundary Conditions, Arrangement of Elements, and Node Point Identification

Two different methods of distributing the mass are also included in this study. The first of these is the generalized mass derived by classical means from the kinetic energy associated with the admissible displacement states (i.e., those assumed in the derivation of the stiffness matrix). The mass matrix thus obtained is the same as the consistent mass matrix derived by Archer, Reference 2, and has the same characteristic population and coupling as the stiffness matrix. The second method of mass distribution studied is the lumped mass distribution in which the total structural mass is divided uniformly into point masses placed at all nodes where translational freedoms are retained. The size of the eigenvalue problem may be reduced by eliminating selected degrees of freedom, retaining those which are considered to be most important in representing the modal response. This reduction is accomplished by the method described by Guyan, (Reference 13). The effect of different degrees of reduction of the original structural freedoms was also examined.

Results of this study are presented in Table 3. Frequencies obtained using both the generalized mass and lumped mass distributions are to be compared with the exact solution of 527 radians per second. The number of elements and the number of total structural degrees of freedom (before reduction) are indicated, as well as the number and identification of degrees of freedom retained (after reduction) in the eigenvalue solution.

Examine first the results obtained with the generalized mass distribution. For one element, with a total of fourteen structural degrees of freedom, very little change is seen in the computed frequency when the number of retained freedoms is reduced from fourteen to five consisting only of the physical translations and rotations at the node points, both results being approximately 2 1/2% high. As further reductions are made, down to three degrees of freedom consisting of the translations at the nodes only, and finally down to one degree of freedom consisting of the normal component of translation only, the error increases to approximately 3 1/2 and 5% respectively. In the four-element idealization, the original 48 structural degrees of freedom are reduced to 12, retaining all translational freedoms, and to four, retaining only the normal translational freedoms, yielding an identical result which is less than 1/2% in error. The nine-element idealization, containing 102 structural degrees of freedom originally, is reduced similarly to 27, retaining all translational freedoms, and then to nine, retaining only the normal translational freedoms, both cases giving the exact solution of 527 radians per second. Finally, the four-element and nine-element idealizations were reduced to one and four degrees of freedom respectively, retaining only the normal translational freedoms at alternate nodes (the subscripts on w in Table 3 refer to the node numbers indicated in Figure 4 which were retained). A sharp increase in the error is noted for both idealizations after this last reduction step. It is apparent that for the same size eigenvalue problem a more accurate and less costly result is obtained by using the next coarser structural idealization and retaining all w freedoms.

TABLE 3

FREQUENCIES CALCULATED FOR CYLINDRICAL SHELL MODE OF FIGURE 3 FROM VARIOUS STRUCTURAL IDEALIZATIONS AND MASS DISTRIBUTIONS

Number and Identification of Retained Freedoms (Mass Points)	NO.	IDENTIFICATION	ω - Radians/Sec (Theory - 527) GENERALIZED MASS	LUMPED MASS
1 Element 14 Structural Freedoms	14	all	539	-
	5	all u, v, w, and β	540	-
	3	all u, v, and w	546	525
	1	all w	552	530
4 Elements 48 Struct. Freedoms	12	all u, v, and w	529	526
	4	all w	529	530
	1	w_9 only	563	500
9 Elements 102 Struct. Freedoms	27	all u, v, and w	527	-
	9	all w	527	531
	4	w_6, w_8, w_{14}, w_{16}	537	524

Examining next the results obtained from the lumped mass distributions given in Table 3, it is apparent that good results were obtained in all cases. This surprising result is due to the fortuitous circumstance or compensating errors, the inherent overstiffness of the stiffness matrix being offset by the apparent increase in flexibility caused by lumping the masses and thereby concentrating the inertial forces.

The same cylinder, Figure 3, has also been analyzed by taking a full quarter of the shell, i.e., a 90-degree sector, in an attempt to obtain all the lower frequency modes in their correct order. Thirty-two elements were used over the quarter of the shell, eight circumferentially and four axially. Antisymmetric boundary conditions were prescribed on the two edges of the 90-degree sector. This eliminates the axial rigid body mode of the cylinder and allows us to obtain the modes having even numbers of waves circumferentially. The results obtained are plotted in Figure 5 as frequency versus the number of circumferential waves, N, for different values of M, the number of axial half-waves, as indicated by the three distinct dashed curves. The corresponding theoretical solutions from Reference 16, are shown as solid curves. This figure shows graphically the decrease in accuracy as the element-size-to-wavelength ratio increases in both the axial and circumferential directions as indicated by increasing values of M and N respectively. Numerically, this error increases from less than one-half percent at M = 1, N = 4, to approximately 18 percent at M = 3, N = 16. The 16 modes obtained from the finite element analysis generally appear in the correct sequence of ascending frequency, although some are interchanged where a higher order mode has a slightly lower frequency than a lower order mode. In these cases, the increased stiffness of the finite element model due to the larger element-size-to-wavelength ratio has caused a greater increase in the error of the finite element analysis between the two modes than the theoretical difference in frequency. For example, in the case of M = 1, the N = 6 and the N = 10 modes are interchanged as are the N = 4 and the N = 14 modes.

The freedoms retained in the quarter shell analysis are the normal displacement component, w, and the rotation, β_θ, at all nodes. Thus, approximately 20% of the original structural degrees of freedom were retained as mass points. The generalized mass distribution described previously was used. The reason for retaining β_θ in this study was to better represent the higher modes having N greater than 8, thus having circumferential element-size-to-wavelength ratios greater than 1:4, as in the coarsest idealization used in the quarter-wave study.

To compare the finite element vibration analysis with experimental results, tests of an unstiffened cylinder with fixed-free boundary conditions, as reported in Reference 17 were selected. The specific model is that referred to as Model 1 in the report and consisted of a circular cylinder 48 inches long, 20 inches in diameter, and 0.03 inches thick, fully clamped

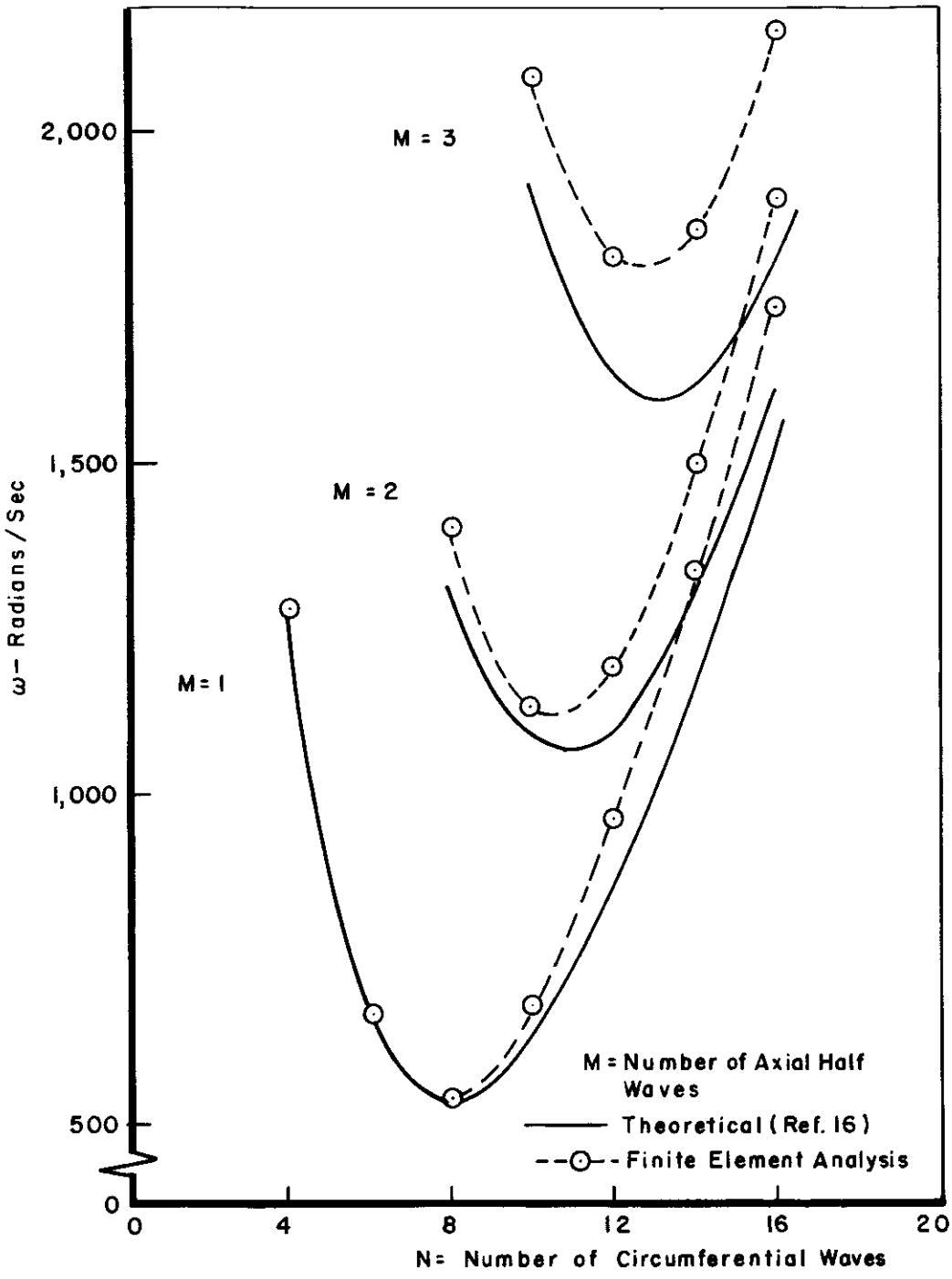

Figure 5. Natural Frequencies of a Circular Cylinder Calculated by Finite Element Analyses Compared With Theory

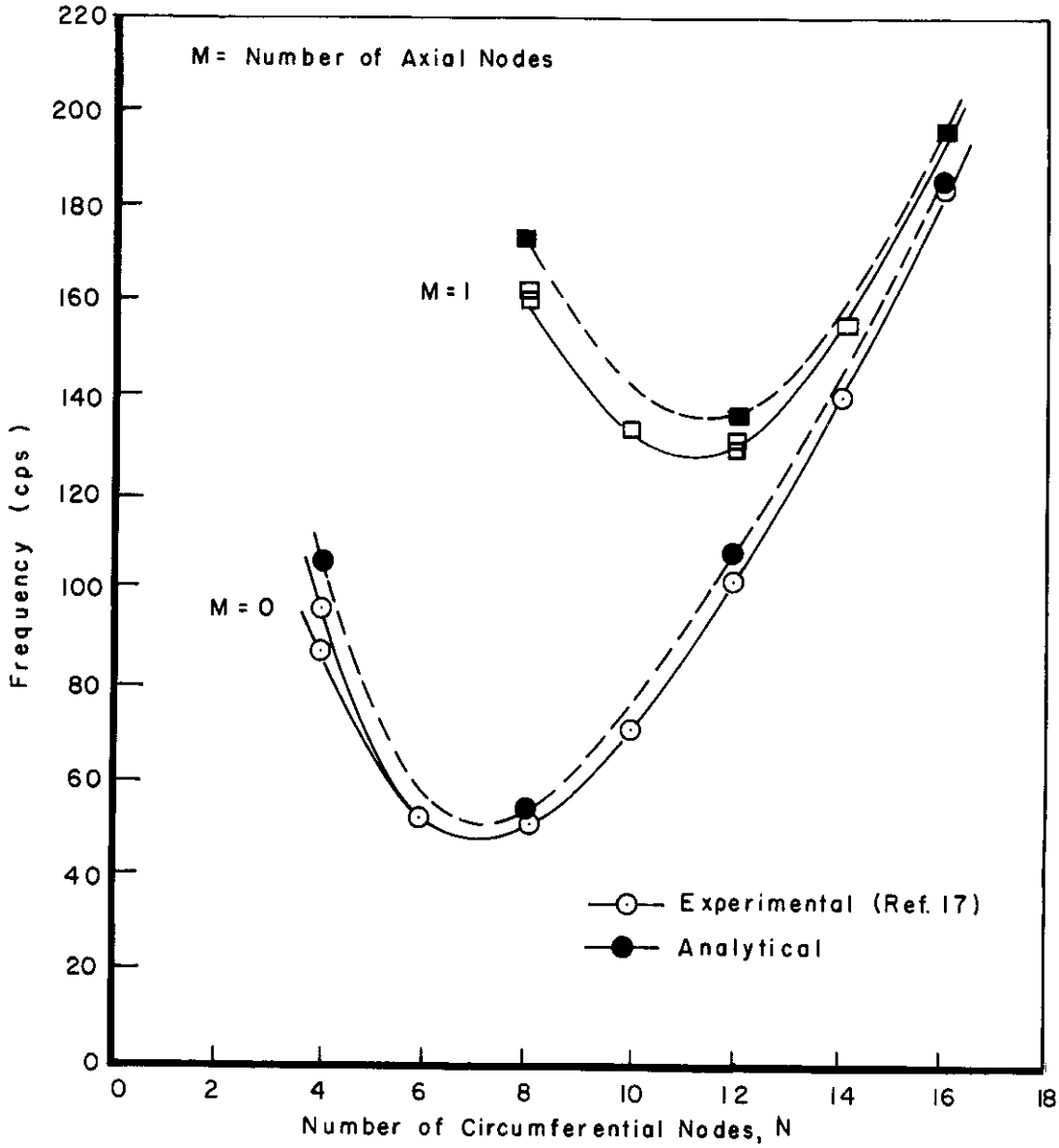

Figure 6. Correlation of Experimental Versus Analytical Results for Vibration of a Fixed-Free Cylindrical Shell

at one end and free at the other. The finite element idealization consisted of 24 elements over one quarter of the shell, four axially and six circumferentially, with symmetric boundary conditions at the edges of the quadrant of the cylinder. The generalized mass distribution with w and β_θ freedoms retained at each node was used. The experimental results from Reference 17 and the first six modes obtained in the finite element analysis are shown in Figure 6. Note that here the definition of M and N differs from that given previously, M being the number of nodes on an axial line (generator) of the cylinder and N being the number of nodes on a circumferential line. Nodes are understood here to be points of zero normal

displacement, w. With the boundary conditions used only modes having even numbers of waves circumferentially are obtained, thus analytical results are plotted only at values of N which are multiples of four.

The correlation is quite good; the increase in error with increase of M and N noted in the correlation with theory is not apparent here. This may be due in part to the fully clamped boundary conditions assumed in the analysis at the fixed end, which probably differ from those actually achieved in the experiment. This might very well influence the experimental frequencies of the lower order modes.

SPHERICAL CAP

Axisymmetrical vibration modes were computed for a ϕ = 60 degrees spherical cap with hinged-fixed boundaries (i.e., zero displacement and moment). The shell and its properties are shown in Figure 7. Calculations were performed for two idealizations and frequencies and mode shapes are compared with theory in Figures 8 to 11.

The spherical cap was idealized by six and ten elements located along the meridian. Since the finite element solutions are compared only with theoretical axisymmetric modes, the shell was idealized by a 15-degree slice with proper boundary conditions along the meridional lines to enforce axisymmetric modal patterns. The six and ten element idealization contained 47 and 97 freedoms, respectively, with the stiffness and mass matrices reduced to 11 and 19 freedoms, respectively, for the eigensolution. Only the normal displacement w was retained as a freedom in the eigensolution with the reduction of mass matrix calculation based on Guyan's method, (Reference 13).

Figures 8 through 11 give the first four theoretical mode shapes and frequencies and the finite element solutions for the two idealizations. The first and second mode shapes are as expected with one and two crossings of the meridional line respectively. The third mode is peculiar in that it does not cross the meridional line (i.e., no interior nodes). This mode is missing in the theoretical solution given by Kalnins, (Reference 18), but was later determined as a proper mode shape by Cohen, (Reference 19). The fourth axisymmetric mode shape contains three interior nodes and corresponds to Kalnins's third and Cohen's fourth mode respectively. Although the ten-element idealization gave excellent results for all modes, the six-element idealization experienced difficulty in determining the third mode shape accurately and was in considerable error on the fourth mode. The excessive stiffening that occurs in the six-element idealization for the higher modes reflects the inadequacy of this idealization to represent the waveforms.

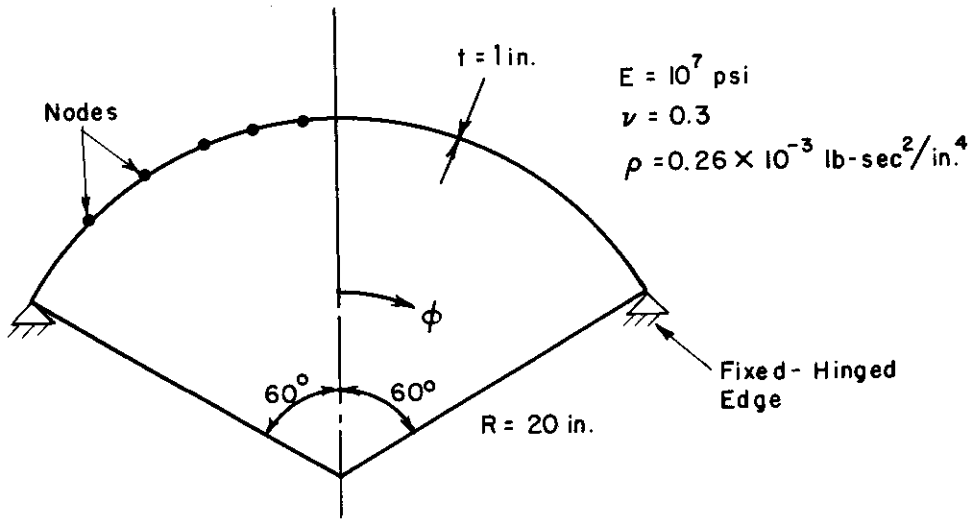

Figure 7. Geometry, Material Properties, and Idealizations - Spherical Cap

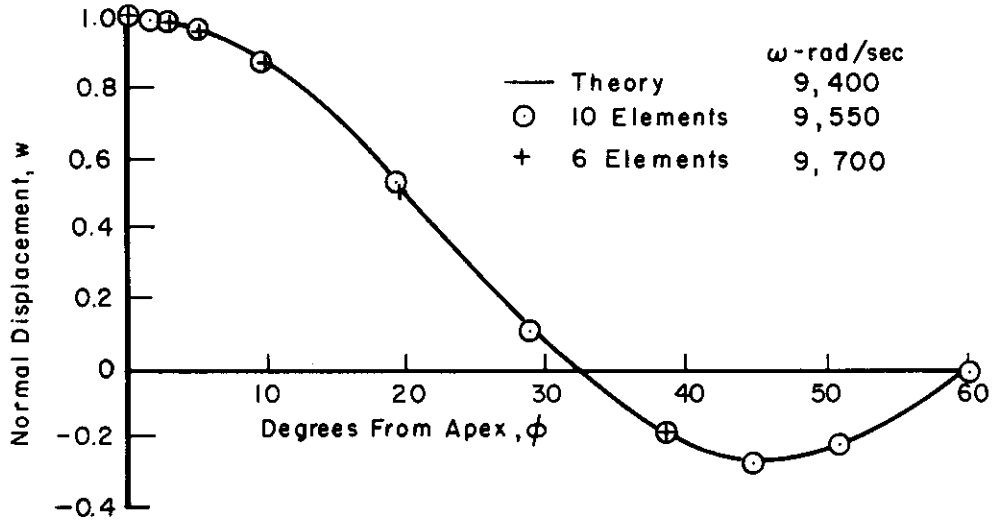

Figure 8. First Axisymmetric Mode Shape - 60° Spherical Cap

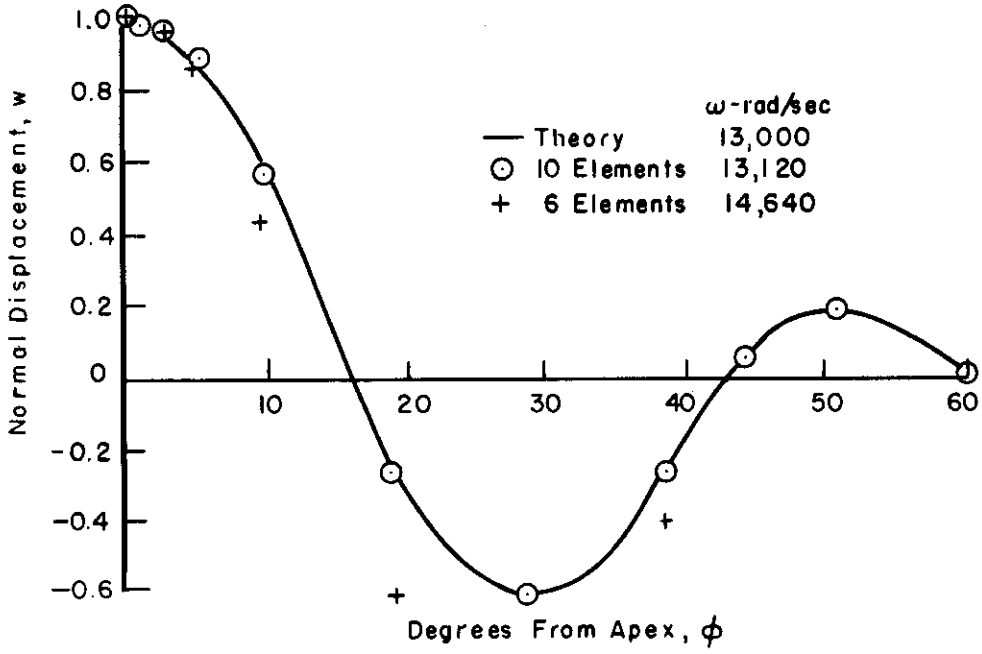

Figure 9. Second Axisymmetric Mode Shape - 60° Spherical Cap

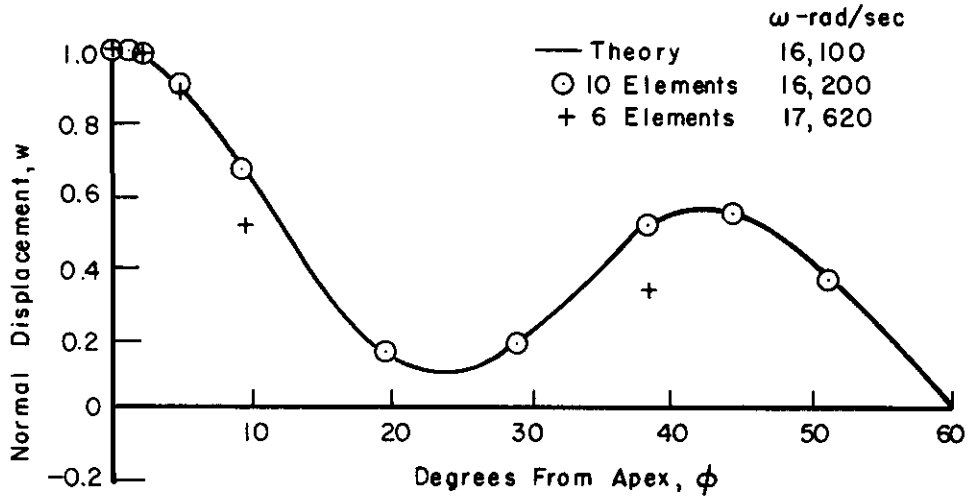

Figure 10. Third Axisymmetric Mode Shape - 60° Spherical Cap

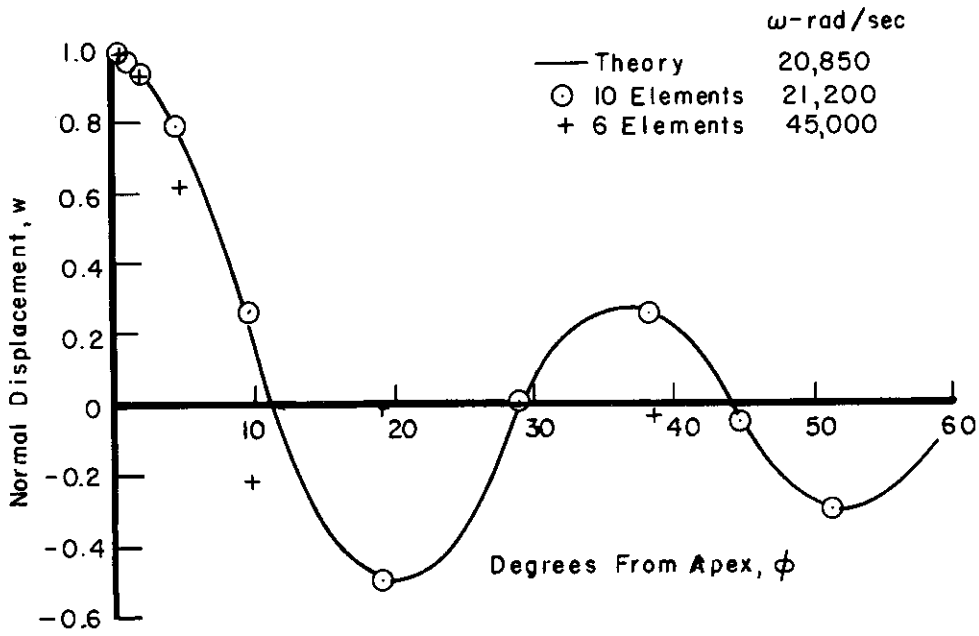

Figure 11. Fourth Axisymmetric Mode Shape - 60° Spherical Cap

SECTION V

CONCLUSIONS

A capability for the dynamic analysis of doubly curved shells by the finite element method has been developed. The derivation of the shell elements and their implementation have been discussed in some detail, with particular emphasis on the choice of displacement functions, the means of approximating the shell geometry, and the extension of the generalized finite element method which is being used in applying the methods to a triangular element. The validity of the methods developed for the quadrilateral shell element has been demonstrated by numerical results. Specifically, these results support the conclusions drawn from previous work that rigid body modes need not be explicitly included in the element displacement functions if the latter are of sufficiently high degree, and that the u, v, and w displacement components should be of equally competent degree. Also supported by the results is the validity of the method adopted for approximating the shell geometry.

The numerical results presented include solutions to both static and dynamic shell response problems. These have led to the following conclusions regarding the usage of the analysis capability developed.

The finite element static results show excellent agreement with theoretical solutions. The hemispherical edge effect problem illustrates the capability of the doubly curved shell elements to determine accurately rapidly varying displacement fields. The curved elements also predict accurately the predominantly membrane behavior for the internally pressurized ellipse.

The dynamic results presented show the effect of the element-size-to-wave-length ratio, and of the different ways of distributing the mass, on the accuracy of the analysis. When the generalized mass distribution is used, the size of the eigenvalue problem may be reduced by the method previously described. As a general rule it appears that good results can be obtained by reducing up to 90% of the original structural freedoms, retaining only the normal translations, w, at each node. Following this procedure, with an element-size-to-wavelength ratio of 1:4, accuracy of better than 5% can be expected in the predicted frequency. The accuracy improves rapidly as the above ratio decreases, but may also deteriorate rapidly as the ratio increases. The latter effect was noted specifically in the case of the axisymmetric modes of the 60-degree spherical cap. With the six-element idealization the error in the frequency of the fourth mode obtained with no reductions was 9%; however, when the 47 original degrees of freedom were reduced to the 11 normal displacements at the nodes (an 80% reduction), the error in frequency increased to 115%. Because of the nature of the mode and the placement of the elements, the element-size-to-wavelength ratio is greater than 1:2 over a large region near the edge of the shell.

The foregoing statements apply to cases where the modal response is of the typical kind in which normal displacements participate significantly. In cases where the modes of interest are of a type in which normal displacements do not participate significantly, e. g., in torsional modes of a cylinder, then u or v displacement components should be retained rather than w. Also, it is presupposed that a sufficient number of elements has been used to represent adequately the geometry of the shell.

The lumped mass distribution, while not elegant in the mathematical sense, nevertheless has certain advantages:

(1) More accurate answers are obtained with a coarser idealization;

(2) Computing time necessary to generate a generalized mass matrix is saved:

(3) Reduction of the mass matrix, which is roughly four times slower than reduction of the stiffness matrix, is unnecessary and considerable computing time is saved.

For this reason it appears that the use of lumped masses in the dynamic analysis of shells is more attractive from the engineering viewpoint.

ACKNOWLEDGMENTS

The authors wish to acknowledge the programming and computing effort of Cliff Durbin, Ronald Thorne, and Leonard Tripp of the Structures Group, Computing and Analysis.

SECTION VI

REFERENCES

1. Novozhilov, V. V., The Theory of Thin Shells, P. Noordhoff Ltd., Groeningen, The Netherlands, 1959.

2. Archer, J. S., "Consistent Mass Matrix for Distributed Mass System," Journal of the Structural Division, ASCE, pp. 161-178, August, 1963.

3. Jones, R. E., Strome, D. R., "Direct Stiffness Method Analysis of Shells of Revolution Utilizing Curved Elements," AIAA J.4, pp. 1519-1525 (1966).

4. Cantin, G., Clough, R. W., "A Refined Curved Cylindrical Shell Finite Element," AIAA Paper No. 68-176, presented at AIAA 6th Aerospace Sciences Meeting, New York, N. Y., January, 1968.

5. Bogner, F. K., Fox, R. L., Schmidt, L. A., "A Cylindrical Shell Element," AIAA J.5, pp. 745-750 (1967).

6. Haisler, W. E., Stricklin, J. A., "Rigid-Body Displacements of Curved Elements in the Analysis of Shells by the Matrix Displacement Method," AIAA J.5, pp. 1525-1527 (1967).

7. Greene, B. E., Jones, R. E., McLay, R. W., Strome, D. R., "On the Application of Generalized Variational Principles in the Finite Element Method," AIAA Paper No. 68-290, presented at AIAA/ASME 9th Structures, Structural Dynamics and Materials Conference, Palm Springs, California, April, 1968.

8. Bogner, F. K., Fox, R. L., Schmidt, L. A., "The Generation of Inter-Element-Compatible Stiffness and Mass Matrices by the Use of Interpolation Formulas," Proceedings of Conference on Matrix Methods in Structural Mechanics, AFFDL-TR-66-80, Wright-Patterson Air Force Base, December, 1965, pp. 397-444.

9. Clough, R. W., Tocher, J. L., "Finite Element Stiffness Matrices for Analysis of Plate Bending," Proceedings of Conference on Matrix Methods in Structural Mechanics, AFFDL-TR-66-80, Wright-Patterson Air Force Base, December, 1965, pp. 515-546.

10. Tocher, J. L., Hartz, B. J., "Higher Order Finite Element for Plane Stress," Journal of the Engineering Mechanics Division, ASCE Vol. 93, No. EM4, pp. 149-172 (1967).

11. Jones, R. E., "A Generalization of the Direct Stiffness Method of Structural Analysis," AIAA J.2, pp. 821-927 (1964).

12. McLay, R. W., "A Special Variational Principle for the Finite Element Method," Technical Note submitted to the AIAA Journal, October, 1968.

13. Guyan, R. J., "Reduction of Stiffness and Mass Matrices," AIAA J.3, p. 380 (1965).

14. Galletly, G. D., "Influence Coefficients for Open-Crown Hemispheres," Journal of Eng. for Industry, Trans. of ASME, pp. 73-81, January, 1960.

15. Galletly, G. D., "Bending of 2:1 and 3:1 Open-Crown Ellipsoidal Shells," Welding Research Council Bulletin Series, No. 54, October, 1959.

16. Voss, H. M., "The Effect of an External Supersonic Flow on the Vibration Characteristics of Thin Cylindrical Shells," JAS, December, pp. 945-961, 1961.

17. Park, A. C., et. al., Dynamics of Shell-Like Lifting Bodies, AFFDL-TR-65-17, Part II. The Experimental Investigation, June, 1965.

18. Kalnins, A., "Free Vibration of Rotationally Symmetric Shells," J. Accoust. Soc. Am., 36, pp. 1355-1365 (1964).

19. Cohen, G. A., "Computer Analysis of Asymmetric Free Vibrations of Ring-Stiffened Orthotropic Shells of Revolution," AIAA J. 3, pp. 2305-2312 (1965).